

pubs.acs.org/JPCA Article

Reactions of Atomic Thorium and Uranium Cations with SF₆ Studied by Guided Ion Beam Tandem Mass Spectrometry

Amanda R. Bubas, Anna C. Iacovino, and P.B. Armentrout*



Cite This: J. Phys. Chem. A 2022, 126, 3239-3246



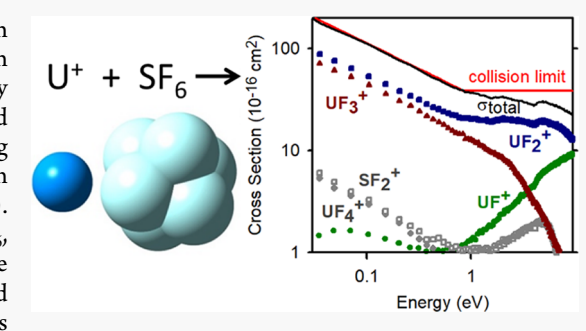
ACCESS

Metrics & More

Article Recommendations

SI Supporting Information

ABSTRACT: The fundamental chemistry of the thorium and uranium fluorides continues to be an area of interest because of the use of thorium and uranium fluoride compounds in nuclear fuel systems. Here, we study the reaction of thorium cations with sulfur hexafluoride for the first time and revisit the reaction of uranium cations with sulfur hexafluoride. By using guided ion beam tandem mass spectrometry, we explore the reaction pathways that become accessible well above thermal energies ($E \sim 0.04 \text{ eV}$). Overall, we find that both Th⁺ and U⁺ react very efficiently with SF₆, approaching the collision limit at both thermal and elevated energies. The primary products observed at low energies include Th₁₋₃⁺, UF₁₋₄⁺, and SF₁₋₄⁺, all of which are formed in barrierless, exothermic processes. SF₅⁺ was



also observed, although the pressure dependence of this channel reveals that SF_5^+ forms exothermically through secondary reactions, which the energy dependences suggest result from reactions between ThF_2^+ and UF_3^+ with SF_6 . At higher energies, both AnF_3^+ products are observed to decay to $AnF^+ + F_2$, and both SF_4^+ and SF_2^+ exhibit cross sections with endothermic features. For both systems, the rise in SF_4^+ can be attributed to a secondary collision between AnF^+ with SF_6 on the basis of the pressure dependence of the SF_4^+ channel at higher energies, and the rise in SF_2^+ appears to result from the decomposition of SF_3^+ to $SF_2^+ + F$.

■ INTRODUCTION

Thorium and uranium fluoride species continue to be studied because of their involvement in the nuclear fuel industry, primarily in liquid fluoride thorium reactors¹ and as uranium hexafluoride in the isotopic enrichment² phase of the nuclear fuel cycle. Fundamental studies of the intrinsic reactivity of these actinyl fluoride species are crucial for the advancement of current nuclear fuel processing technologies and the safe handling and storage of nuclear fuel and to develop effective solutions to contamination issues that may arise.

A number of studies have aimed at gathering fundamental thermodynamic information for the thorium and uranium fluorides.^{3,4} High-temperature mass spectrometry (HTMS) experiments by Hildenbrand and coworkers were conducted to measure threshold appearance energies of the thorium fluoride and uranium fluoride cations, as well as equilibrium constants for many reactions that form neutral thorium fluoride and uranium fluoride species. 5-7 The measured values were used to derive reaction enthalpies, entropies, and bond dissociation energies (BDEs). Heaven and co-workers determined precise values for the ionization energies (IEs) and BDEs of the monofluorides of both thorium and uranium.^{8,9} The IEs and electronic structures of ThF4 and UF4 have been determined and detailed by photoelectron spectroscopy. 10 High-level coupled-cluster with single, double, and perturbative triple excitations, CCSD(T), calculations have been performed to compute heats of formation and BDEs for neutral and ionic thorium fluorides ThF₁₋₄ and ThF₁₋₄. We have previously evaluated and compiled this thermodynamic information for $\operatorname{AnF}_n^{+/0}$ (n=1-4) where $\operatorname{An}=\operatorname{Th}$ and U^{12} The thermodynamic values included in this earlier publication follow the thermal electron convention for ionic heats of formation. As detailed by Bartmess, 13 the assumption of Boltzmann statistics and addition of 6.1973 kJ/mol to account for the enthalpy of an electron at 298.15 K are incorrect. Electrons are fermions and therefore need to be described using Fermi–Dirac statistics; therefore, the ion heats of formation listed in this prior publication are consistently 3.051 kJ/mol too high. Here, Table 1 includes comparable information for $\operatorname{UF}_n^{+/0}$ (n=5 and 6) from Hildenbrand and coworkers 7,14 following the Fermi–Dirac electron convention.

Thermodynamic data for SF_n and SF_n^+ (n=1-5) species remain uncertain. ¹⁵⁻¹⁷ Heats of formation from the JANAF tables ¹⁶ have largely been supplanted by more recent studies. These include studies of the collision-induced dissociation and charge transfer of the cations using a guided ion beam tandem mass spectrometer (GIBMS) by Fisher et al. ¹⁷ In retrospect, the IEs measured in this work have proven robust, as have the

Received: March 26, 2022 Revised: April 27, 2022 Published: May 11, 2022





Table 1. Thermochemical Values at 0 (Italics) and 298 (Normal) K (Uncertainties in Parentheses)

species	$\Delta_f H$ (A) (kJ/mol)	$D(F_{n-1}An-F)$ (kJ/mol)	IE (A) (eV)	$\Delta_f H (A^+) (kJ/mol)$	$D(F_{n\text{-}1}An^{\text{+}}\text{-}F) \ (kJ/mol)$
UF ₅	$-1929 (10)^a$	410 (6) ^a	$11.29 (0.10)^{b}$	$-836 (15)^c$	303 (33) ^c
UF_6	$-2147 (2)^a$	$297 (8)^a$	$14.00 (0.10)^{b}$	$-793 (13)^c$	$36 (20)^c$
F	$77.28, 79.39 (0.30)^d$		17.42282 ^e	$1758.33, 1763.78 (0.30)^d$	
S	$274.73, 276.98 (0.25)^d$		10.36001 ^e	$1274.31, 1279.24 (0.40)^d$	
SF	12 (6) ^f , 12 (6) ^g	340 (6) ^f	$10.32 \ (0.02)^{f,h}$	$1008 (5)^{f,i}$, $1011 (5)^g$	$343 (5)^{f,i}$
	3.5, 3.0 ^j	346.4, 350.0 ^j	10.25 ^c	992.2, 995.3 ^j	359.4, 363.3 ^j
SF_2	$-290 \ (12)^{f,i}, \ -293 \ (12)^g$	380 (13) ^f	$10.08 \ (0.05)^{e,f}$	683 (11) ^{f,i} , 684 (11) ^g	$402 (10)^{f,i}$
	$-292.2, -295.2^{j}$	373.0, 377.6 ^j	10.17^{c}	689.4, 690.3 ^j	380.1, 384.3 ^j
SF_3	$-431 (21)^f$, $-435 (21)^g$	218 (23) ^f	$8.18 \ (0.07)^{f,i}$	358 (21) ^f , 356 (21) ^g	402 (23) ^f
	$-437.3, -441.6^{j}$	222.3, 225.9 ^j	8.26 ^c	359.7, 358.0 ^j	407.0, 411.7 ^j
SF_4	$-757 (21)^{f,i}, -764 (21)^g$	403 (9) ^f	11.90 (0.03) ^f	389 (21) ^f , 386 (21) ^g	$35 (5)^{f,i}$
	$-760.9, -768.4^{j}$	401.0, 406.2 ^j	11.92^{c}	389.4, 386.2 ^j	47.6, 51.2 ^j
SF ₅	$-849 (9)^k, -859 (9)^g$	182 (25) ^{f,k}	$9.60 \ (0.05)^{f,i,l}$	77 (8) ^k , 70 (8) ^g	402 (26) ^{f,k}
	-837.0, -846.6 ^j	153.3, 157.6 ^j	9.55 ^c	84.1, 77.5 ^j	382.6, 388.1 ^j
SF ₆	$-1206.50, -1220.47 (0.8)^d$	369 (14) ⁱ 446.9, 453.3 ^j			

"Ref 7. "Ref 14. "Derived value using $\Delta_t H(A^+) = \Delta_t H(A) + IE + 1.27 \ k_B T$ (3.146 kJ/mol at 298.15 K, Fermi-Dirac electron convention) or $D(F_{n-1}An^{0/+}-F) = \Delta_t H(F_{n-1}An^{0/+}) + \Delta_t H(F) - \Delta_t H(AnF_n^{0/+})$. "Ref 16. "Ref 15. "Ref 20. "Thermal corrections from Bauschlicher added to 0 K values from Ng. "Does not appear to be a direct experimental measurement but is derived from the experimental heats of formation of SF and SF*. "Ref 17. "Ref 24. "Ref 21. "Ref 22."

cationic BDEs for the smaller values of n (1 and 2), whereas BDEs for larger values of n tend to be too high. This is probably a consequence of not including an explicit evaluation of kinetic shifts, which at that time was not the routine tool developed later. Some time later, Ng and co-workers evaluated the available experimental data by comparison with G2 calculations to provide recommended experimental values.²⁰ These values are adopted in Table 1 for n = 1-4species of both the neutrals and cations. Subsequently, Ng and co-workers²¹ made a more definitive measurement of the 0 K heat of formation of SF₅, $\Delta_t H_0(SF_5)$, which they combined with an ionization energy (IE) for SF₅ from Sieck and Ausloos²² and Fisher et al.¹⁷ to obtain $\Delta_t H_0(SF_5^+)$. These values are also provided in Table 1. At about the same time, two complementary theoretical studies were performed by Irikura, ²³ using empirically corrected G2 and G2(MP2) values, and Bauschlicher and Ricca,²⁴ who performed CCSD(T)/ CBS//B3LYP calculations (where CBS is a complete basis set extrapolation). These two studies yield very similar results. Those of Bauschlicher and Ricca are listed in Table 1 as this higher level of theory yields values in slightly better agreement with the experimental values. For this thermochemistry, atomization energies and bond energies calculated by Bauschlicher and Ricca were converted to heats of formation relative to experimental heats of formation for SF₆ for the neutrals and S⁺ + nF for the ions. Oddly, the ionization energies listed by Bauschlicher and Ricca do not reproduce the differences in the heats of formation of the neutrals and ions at 0 K. It appears that the calculated IE values were systematically and inappropriately reduced by 2.48 kJ/mol (= k_BT at T = 298.15 K). Values for the theoretical IEs listed in Table 1 are calculated from the heats of formation at 0 K listed by Bauschlicher and Ricca. Heats of formation for the ions listed in Table 1 follow the Fermi-Dirac electron convention. Although left unstated, 298 K values for ions from Bauschlicher and Ricca appear to have utilized the thermal electron convention; therefore, the 298 K values cited by Bauschlicher and Ricca have been reduced by 3.051 kJ/mol.

The reaction of uranium cations with SF₆ has been previously studied in an ion trap mass spectrometer by Jackson et al.²⁵ The total pseudo-first-order reaction rate and reaction efficiency along with branching ratios were determined. This same study also included an examination of the reactions of UF⁺, UF₂⁺, and UF₃⁺ with SF₆ and H₂O to provide reaction rates, efficiencies, and branching ratios of the observed chemistry. Here, we revisit the reaction of atomic uranium cations with SF₆ using a GIBMS to enable the examination of this reaction beyond the thermal energies accessible in an ion trap instrument. In addition, we examine the analogous reactions of atomic thorium cations with SF6, which have not yet been reported. Reaction rates, efficiencies, and branching ratios were determined for both reactions, and results for the uranium cations reacting with SF₆ are compared to the thermal energy results obtained in the ion trap study.

EXPERIMENTAL METHODS

Instrument. The GIBMS involved in the current work has been previously described in detail. Therefore, only a brief overview is provided here. A DC discharge ionization source was used to generate thorium and uranium ions from the metal cathode of interest. The ions underwent $\sim 10^5$ thermalizing collisions with helium/argon (90:10 mixture) flow gases in the 1 m flow tube region before exiting the source. The ions generated in this source can be characterized by an electronic state distribution that corresponds to a temperature of 700 \pm 400 K, as determined previously. Therefore, the Th⁺ and U⁺ ions are expected to have average electronic energies of 0.02 ± 0.03 and 0.03 ± 0.02 eV, respectively. 34,35

After exiting the source, ions were accelerated through a series of focusing lenses and passed through the magnetic momentum analyzer for reactant ion selection of ²³²Th⁺ and ²³⁸U⁺. Another series of focusing lenses followed to refocus and decelerate the mass-selected precursor ions to well-defined kinetic energies and inject them into a radio frequency (rf) octopole ion beam guide, ^{36,37} which radially traps the ions leading to efficient product ion collection. The octopole guide passes through a much shorter collision cell of effective length

Table 2. Thermochemistry for Reactions of An⁺ with SF₆ at 298 K, Δ_rH₂₉₈ (kJ/mol)

products	Th^a	U^b
$AnF^+ + SF_5$	$-208 \pm 13 \ (-213 \pm 14)$	$-196 \pm 16 \; (-277 \pm 29)$
$AnF^+ + SF_3 + F_2$	$216 \pm 23 \ (192 \pm 14)$	228 ± 25
$AnF_2^+ + SF_4$	$-774 \pm 38 \ (-726 \pm 14)$	$-600 \pm 38 \ (-605 \pm 33)$
$AnF_3^+ + SF_3$	$-999 \pm 38 \ (-975 \pm 14)$	$-729 \pm 26 \ (-789 \pm 18)$
$AnF_4^+ + SF_2$	$-813 \pm 14 \ (-789 \pm 14)$	$-819 \pm 32 \ (-885 \pm 8)$
$UF_5^+ + SF$		$-738 \pm 18 \; (-739 \pm 17)$
$UF_6^+ + S$		-430 ± 15
$SF_5^+ + AnF$	$101 \pm 13 \ (95 \pm 14)$	118 ± 15
$SF_5^+ + ThF_3 + SF_4$	$-639 \pm 26 \ (-626 \pm 14)$	
$SF_5^+ + UF_4 + SF_3$		-657 ± 24
$SF_4^+ + AnF_2$	$-205 \pm 24 \ (-195 \pm 14)$	$-51 \pm 25 \ (-24 \pm 16)$
$SF_4^+ + AnF_3 + SF_5$	$-418 \pm 27 \ (-395 \pm 14)$	-229 ± 26
$SF_3^+ + AnF_3$	$-809 \pm 25 (-797 \pm 14)$	$-621 \pm 25 (-574 \pm 11)$
$SF_2^+ + AnF_4$	$-1069 \pm 13 \ (-1058 \pm 14)$	$-829 \pm 15 \ (-806 \pm 9)$
$SF_2^+ + F + AnF_3$	$-402 \pm 17 \ (-386 \pm 14)$	-213 ± 17
$SF_2^+ + UF_5 + SF_5$		-797 ± 19
$SF^+ + UF_5$		$-832 \pm 14 \ (-854 \pm 14)$
$SF^+ + AnF_3 + F_2$	$-154 \pm 14 \; (-160 \pm 14)$	34 ± 14
$SF^+ + AnF_4 + F$	$-662 \pm 9 (-674 \pm 14)$	-422 ± 11

"Values derived from experimental values in Table 1 and a prior compilation in Ref 12 (computationally derived values from Ref 11). ^bValues derived from experimental values in Table 1 and a prior compilation in Ref 12 (values taken from Ref 25).

 $8.26~\rm cm.~SF_6$ was introduced into the collision cell for reaction with the Th⁺ and U⁺ precursor ions. The pressure was kept sufficiently low that single-collision conditions generally apply; however, data were collected at pressures of about 0.05, 0.1, and 0.2 mTorr to enable extrapolation to zero-pressure, rigorous single-collision conditions. A focusing stage following the octopole extracted the precursor and product ions for subsequent mass analysis by a quadrupole mass filter and detection using a Daly-type detector. 39

Data Analysis. Several factors were considered in data collection and analysis and have been described previously.³⁷ A retarding energy analysis curve was obtained by varying the DC voltage of the octopole through the nominal zero of the ion kinetic energy and monitoring signal intensity. The first derivative of the resulting curve provided the ion beam energy distribution, and the location of the peak in this distribution established the absolute zero of the energy scale. Full widths at half-maximum (FWHMs) of the ion energy distribution were typically 0.5–0.6 eV (Lab), and uncertainties in the absolute energy scale were 0.1 eV (Lab). Lab frame energies were converted to center-of-mass frame energies using the equation $E_{\rm CM} = E_{\rm Lab} \times m/(m+M)$, where m is the mass of the neutral SF₆ reagent and M is the mass of the precursor ion.

Foreground scans were collected with the neutral reagent directed to the collision cell, and background scans were collected with the neutral reagent directed to the chamber surrounding the collision cell, allowing the ion signal resulting from the reaction to be measured and the background noise and signal from collisions outside of the collision cell to be explicitly subtracted. Product ion intensities were corrected for this background and converted to cross sections, σ , using the equation $I = I_0 \exp\left(-\rho\sigma l\right)$, where I is the intensity of the precursor ion after the reaction, I_0 is the precursor intensity before the reaction (assumed to equal $I + \Sigma I_{\rm p}$ where $I_{\rm p}$ are intensities of the various product ions), ρ is the density of the neutral reactant, and l is the length of the collision cell. Uncertainties in the absolute cross section magnitudes are $\pm 20\%$.

Rate constants were obtained by multiplying the cross section by the relative reactant velocity, $\nu = (2E/\mu)^{1/2}$, where μ is the reduced mass of the reactants, and integrating over a Maxwell–Boltzmann distribution, as shown in eq 1.³⁷

$$k(T) = \left(\frac{1}{\pi\mu}\right)^{1/2} \left(\frac{2}{k_{\rm B}T}\right)^{3/2} \int E\sigma(E)e^{-E/k_{\rm B}T} dE$$
 (1)

Reaction efficiencies were calculated by comparing the observed reaction rate constants to the Langevin–Gioumousis–Stevenson $(LGS)^{40,41}$ collision rate, where the polarizability of SF₆ used was 4.49 Å^{3.42}

RESULTS

The thermochemistry for all reactions studied here is listed in Table 2 and derived from values provided in Table 1 and previously tabulated for AnF_n^+ (n = 1-4).¹²

 $\mathsf{Th}^+ + \mathsf{SF}_6$. Figure 1 shows the product ion cross sections as a function of ion kinetic energy for the reaction of Th^+ and SF_6 . The total cross section can be seen to decrease with increasing energy, following the behavior predicted by the LGS model very closely. At higher energies, starting near 1 eV, the total cross section levels out, which we attribute to an approach toward a hard-sphere-like behavior, discussed more quantitatively below.

Looking at the individual product cross sections, it can be seen that cross sections for all products, ThF_{1-3}^{+} and SF_{1-5}^{+} , decline with increasing energy up to about 1 eV, indicating that they are all formed in exothermic, barrierless reactions. These results are consistent with the thermochemistry listed in Table 2 for all reactions except the formation of SF_5^{+} + ThF_7 , an exception discussed further below. Clearly, the transfer of multiple fluorine atoms from the sulfur center to the metal is facile as ThF_3^{+} and ThF_2^{+} , formed in nearly equal amounts, are the dominant products.

At higher energies (>1 eV), the ThF₂⁺ cross section levels out, paralleling the behavior of the total cross section, whereas

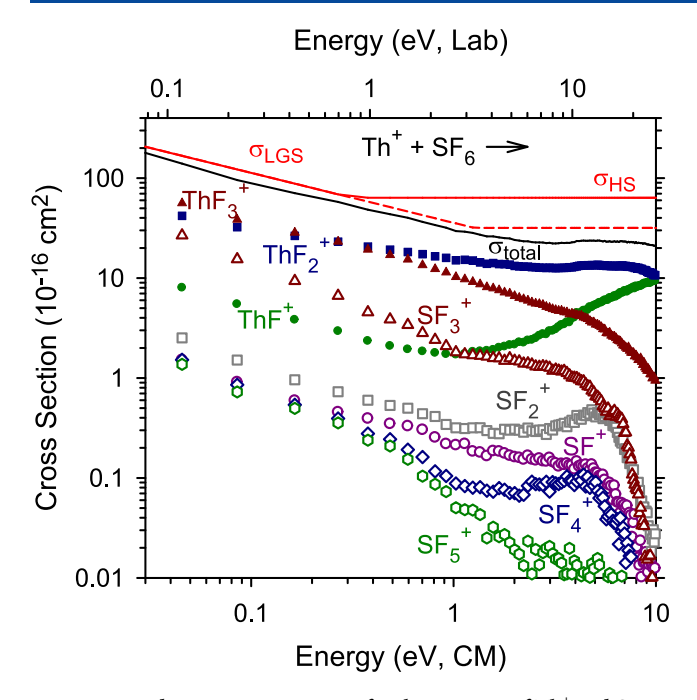


Figure 1. Product ion cross sections for the reaction of Th⁺ and SF₆ at a pressure of 0.2 mTorr as a function of center-of-mass frame (lower axis) and lab frame (upper axis) energies. Closed symbols show ThF_n⁺ product ions and open symbols show SF_{6-n}⁺ ions, with complementary products having the same color. The full line shows the total cross section compared to the collision limit (red line), with the dashed red line showing half of the the hard-sphere cross section.

the ThF $_3^+$ cross section continues to decline. As this occurs, the ThF $_3^+$ cross section increases such that the sum of the ThF $_3^+$ and ThF $_3^+$ cross sections would again parallel the behavior of the total cross section. These complimentary features can be attributed to the decomposition of ThF $_3^+$ to ThF $_3^+$ + F $_2$. As shown in Table 2, the overall formation of ThF $_3^+$ to ThF $_3^+$ + F $_2$ is endothermic by 216 \pm 23 kJ/mol (2.24 \pm 0.24 eV), consistent with the observed behavior. Notably, the similar process for the primary ThF $_2^+$ product (Th $_3^+$ + SF $_4$ \rightarrow ThF $_3^+$ + SF $_4$ \rightarrow ThF $_3^+$ + F $_2$ + SF $_4$) is endothermic by 456 \pm 21 kJ/mol (4.73 \pm 0.22 eV), explaining why the ThF $_3^+$ product does not exhibit the same behavior as the ThF $_3^+$ cross section.

At low energies, all five SF_n^+ product cross sections decline with increasing energy, consistent with the exothermicities listed in Table 2 for the reaction concomitantly forming the ThF_{6-n} neutral; however, the SF⁺ product cannot be accompanied by ThF₅ as this species is not stable. Hence, the formation of SF^+ is probably accompanied by $ThF_4 + F$ or ThF₃ + F₂, which is exothermic by 662 ± 9 and 154 ± 14 kJ/ mol. At higher energies, the SF+, SF3+, and SF5+ cross sections decline monotonically, whereas the SF_2^+ and SF_4^+ cross sections exhibit an increase in magnitude. For SF₂⁺, the only species with a cross-section magnitude large enough to account for the increase in the SF_2^+ cross section is SF_3^+ . Here the overall reaction to form $ThF_3 + SF_2^+ + F$ (i.e., F atom loss from the primary SF_3^+ product ion) is exothermic by $402 \pm 17 \text{ kJ/}$ mol (4.17 \pm 0.18 eV). Even though exothermic, this process could appear at higher energies if the ThF3 product carries away sufficient energy. For the formation of SF₄⁺ at higher energies, the decomposition of the SF₅⁺ product cannot explain this behavior because the SF5+ cross section is too small to account for the increase observed. However, the SF₄⁺ channel cross section is found to be pressure dependent, as shown in

Figure S1. Upon extrapolation to zero pressure, the lowenergy, exothermic reactivity in the SF₄⁺ cross section is retained, but the high-energy, endothermic feature disappears. Such a pressure dependence in the cross section indicates that a secondary reaction of a primary ion with SF₆ is contributing to the formation of SF₄⁺ at all energies. Here, a likely candidate given the endothermic feature is a reaction of ThF+ (formed in both the primary reaction with SF₅ at low energies and the fragmentation process with SF3 + F2 at higher energies) to yield SF₄⁺ + ThF₃. The secondary reaction is exothermic by 210 ± 25 kJ/mol such that the secondary reactions have cross sections that approximately parallel the ThF+ cross section. Finally, we note that the decline in the SF_n⁺ cross sections at the highest energies (above \sim 7 eV) may be associated with these product ions no longer being transmitted efficiently through the quadrupole mass filter. Such an effect may occur if most of the momentum in the laboratory frame is retained by the products containing the heavy Th atom.

Another way to examine the behavior observed in this system is to compare the cross-section intensities of complementary ion pairs, i.e., $ThF_n^+ + SF_{6-n}$ versus $ThF_n +$ SF_{6-n} . Their relative intensities are expected to be consistent with the relative ionization energies (IEs). For example, the ThF₃⁺ cross section is larger than the SF₃⁺ cross section by a factor of \sim 3, consistent with ThF₃ possessing the lower IE (6.2 \pm 0.3 eV⁶) compared to IE(SF₃) = 8.18 \pm 0.07 eV.^{17,20} The same can be said for the ThF2+ and SF4+ ion pair where $IE(ThF_2) = 6.0 \pm 0.3 \text{ eV}^6 < IE(SF_4) = 11.90 \pm 0.03 \text{ eV}^{.20} \text{ Now}$ the larger difference in IEs leads to a larger ratio (\sim 30) than in the ThF₃⁺/SF₃⁺ pair. The ThF⁺ and SF₅⁺ cross sections also show relative magnitudes consistent with their relative IEs, $IE(ThF) = 6.3952 \pm 0.0004 \text{ eV}^9 < IE(SF_5) = 9.60 \pm 0.05$ eV, 17,20,22 but as discussed next, the SF $_5^+$ product is not actually formed in competition with ThF+ + SF₅.

As noted above, literature thermochemical values suggest that the formation of SF₅⁺ + ThF is endothermic. An examination of the SF₆ pressure dependence of the SF₅⁺ product channel, shown in Figure S2, reveals that the magnitude of the SF5+ product ion cross section increases with increasing SF₆ pressure. A linear extrapolation to zero pressure, i.e., single-collision conditions, reduces the magnitude of this product to zero within experimental uncertainty at all energies, demonstrating that this species is formed through a secondary reaction. There are multiple secondary processes leading to SF₅⁺ that are exothermic starting with Th⁺ + 2SF₆ reactants. A likely candidate was located by assuming that the secondary formation of SF₅⁺ occurs via an exothermic reaction and therefore has an energy dependence provided by the LGS cross section, i.e., $E^{-1/2}$. After adjusting for this $E^{-1/2}$ additional energy dependence, the shape of the SF5+ cross section was compared to the primary cross sections and closely matches the energy dependence of the ThF2+ product cross section. Further, the magnitude of the large ThF₂⁺ cross section exhibits a mild decrease with increasing SF₆ pressure, consistent with a secondary reaction between ThF₂⁺ and SF₆. The overall reaction, $Th^+ + 2SF_6 \rightarrow SF_5^+ + ThF_3 + SF_4$, is exothermic by 639 \pm 26 kJ/mol, consistent with our observations. Notably, the secondary reaction involved here, $ThF_2^+ + SF_6 \rightarrow SF_5^+ + ThF_3$, is endothermic by 135 \pm 34 kJ/ mol, indicating that some of the 774 \pm 38 kJ/mol exothermicity of the ThF2+ + SF4 formation is retained by the ThF₂⁺ product.

 $U^+ + SF_6$. The product ion cross sections for the reaction of U^+ and SF_6 are shown in Figure 2. The total cross section

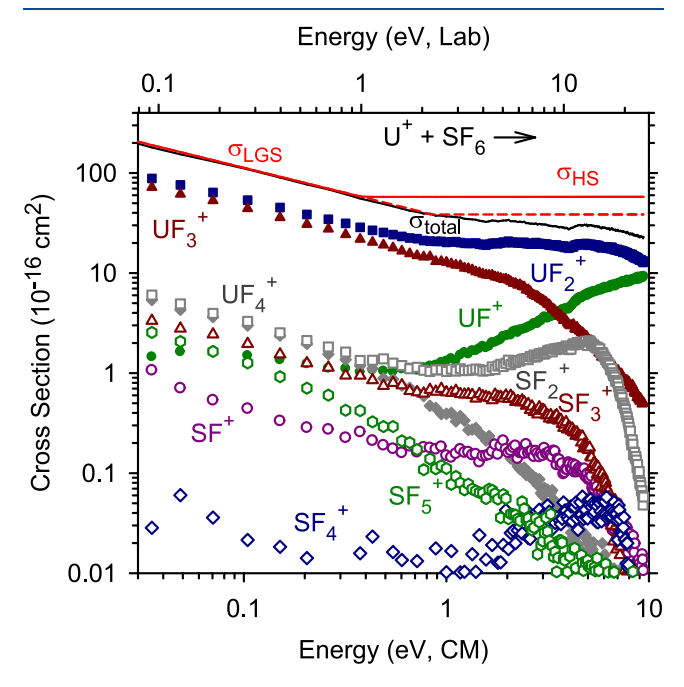


Figure 2. Product ion cross sections for the reaction of U^+ and SF_6 at a pressure of 0.2 mTorr as a function of center-of-mass frame (lower axis) and lab frame (upper axis) energies. Closed symbols show UF_n^+ product ions and open symbols show SF_{6-n}^+ ions, with complementary products having the same color. The full line shows the total cross section compared to the collision limit (red line), with the dashed red line showing two-thirds of the hard-sphere cross section.

decreases with increasing energy up to \sim 1 eV and is nearly superimposable with the LGS model. At higher energies, the total cross section remains constant, a feature attributed to the approach toward the hard-sphere collision limit.

All individual product ion cross sections decrease with increasing energy up to ~ 1 eV, indicating that the observed UF₁₋₄⁺ and SF₁₋₅⁺ products form through exothermic, barrierless reactions, which are consistent with the thermochemistry listed in Table 2 for all products except SF₅⁺ + UF. Analogous to observations made for the reaction of thorium cations and SF₆, UF₂⁺, and UF₃⁺ formation are the dominant processes, illustrating that multiple fluorine atom transfers are facile.

At higher energies, the UF2+ cross section levels out and closely resembles the shape of the total cross section. In contrast, after 1 eV, the UF3+ cross section decreases, while the UF+ cross section increases. A likely explanation of these complimentary features is the decomposition of UF₃⁺ to UF⁺ + F_2 , for an overall reaction of $U^+ + SF_6 \rightarrow UF^+ + SF_3 + F_2$ which is endothermic by 228 \pm 25 kJ/mol. Likewise, as was observed for the reaction of Th^+ and SF_6 , the SF_2^+ and SF_4^+ cross sections both increase beginning near 1-2 eV. In apparent contrast to the Th system, the increase in the SF₂⁺ cross section does not appear to result from the decomposition of SF₃⁺ as the cross section for the latter is too small; however, the SF₂⁺ and SF₃⁺ channels display a pressure dependence, shown in Figures S3 and S4. For SF₂⁺ and SF₃⁺, the zeropressure extrapolated cross sections parallel those shown in Figure 2, but SF_2^+ is smaller by about a factor of 2–3, whereas SF₃⁺ is larger by the same factor. This result is consistent with SF_3^+ decomposing to SF_2^+ , as also observed for the thorium system. This is plausible as the overall reaction forming $SF_2^+ + F + UF_3$ is exothermic by 213 \pm 17 kJ/mol, although the pressure dependence suggests that a secondary collision helps augment this additional fragmentation process. Similarly, we find that the SF_4^+ cross section is pressure-dependent at all energies, as shown in Figure S5, and therefore is produced in a secondary reaction. Although not efficient, UF^+ (formed both at low energies with SF_5 and at high energies with $SF_3 + F_2$) can react further with SF_6 to form $SF_4^+ + UF_3$. The secondary reaction is slightly exothermic, by 34 \pm 25 kJ/mol, such that the SF_4^+ cross section follows the shape of the UF^+ precursor.

Also, as for the thorium system, the declines in the SF_n^+ cross sections at the highest energies (above \sim 7 eV) may be associated with no longer being transmitted efficiently through the quadrupole mass filter because products containing the heavy U atom retain most of the momentum in the laboratory frame. Here, such behavior is particularly evident in the very sharp decline observed in the SF_4^+ cross section. As none of the rest of the SF_n^+ cross sections here or in the Th system behave this precipitously, their cross sections may be accurate at high energies.

Similar to observations made for the reaction of Th⁺ and SF₆, complementary product ion cross-section magnitudes for the reaction of U⁺ and SF₆ are consistent with the relative IEs listed in Table 1 and previously. For example, the UF₃⁺ cross-section magnitude is greater than that for the SF₃⁺ product by a factor of ~8, in agreement with IE(UF₃) = 7.05 \pm 0.10 eV 5 < IE(SF₃) = 8.18 \pm 0.07 eV. Table 17.20 Likewise, for the UF₂⁺/SF₄⁺ pair where the IE difference is much larger, IE(UF₂) = 6.2 \pm 0.3 eV 5 < IE(SF₄) = 11.90 \pm 0.03 eV, the UF₂⁺ cross section exceeds that for SF₄⁺ by more than 3 orders of magnitude (~1800). For the UF₄⁺/SF₂⁺ complementary product pair, where IE(UF₄) = 10.2 \pm 0.3 eV and IE(SF₂) = 10.08 \pm 0.05 eV 15,20 are very similar, the SF₄⁺ cross section is only greater than the UF₂⁺ cross section by a factor of ~1.5.

As for the thorium system, the reaction thermochemistry detailed in Table 2 suggests that the formation of SF₅⁺ + ThF is endothermic. Analysis of the SF₆ pressure dependence of the SF₅⁺ cross section, shown in Figure S6, confirms that SF₅⁺ forms through a secondary collision. Again, the SF₅⁺ cross section was adjusted for an $E^{-1/2}$ dependence and compared to the primary cross sections. The shape of the UF₃⁺ cross section exhibited the closest match, providing support that SF5+ forms through a secondary reaction between UF3+ and SF6 for an overall reaction, $U^+ + 2SF_6 \rightarrow SF_5^+ + UF_4 + SF_3$, which is exothermic by 657 ± 24 kJ/mol. The secondary reaction is endothermic by 71 \pm 17 kJ/mol, which is consistent with observations of Jackson et al. that UF3+ was inert to the reaction with SF₆ at thermal energies. In the near singlecollision conditions utilized in the GIBMS experiments, the UF₃⁺ product formed in the primary reaction can retain some of the 729 \pm 26 kJ/mol exothermicity, helping to drive the secondary process.

Finally, we note that the thermochemistry in Table 2 indicates that formations of $UF_5^+ + SF$ and $UF_6^+ + S$ products are exothermic, but neither product channel was observed. This could be a result of the kinetic difficulty of transferring five or six fluorine atoms during the lifetime of the transient $AnSF_6^+$ collision complex.

DISCUSSION

ThF₁₋₃⁺ and UF₁₋₄⁺ Channels. We measure that the reactions of Th⁺ and U⁺ + SF₆ proceed at rates of $4.5 \pm 0.9 \times 10^{-10}$ and $5.1 \pm 1.0 \times 10^{-10}$ cm³ s⁻¹, respectively, at thermal energies. When compared to the Langevin-Gioumousis-Stevenson (LGS) 40,41 rate constant of 5.2 × 10 $^{-10}$ cm 3 s $^{-1}$, these reactions proceed with efficiencies (k/k_{LGS}) of 0.87 \pm 0.17 and 0.98 ± 0.20 , respectively. In these systems, the exothermicities of the reactions permit the facile transfer of multiple fluorine atoms from the sulfur to the actinide center. The dominance of the AnF₂⁺ and AnF₃⁺ over AnF⁺ products is consistent with the lower exothermicity of the latter channel. In contrast, even though the transfer of four fluorine atoms is also strongly exothermic (Table 2), this process is not observed in the thorium system and is about an order of magnitude less probable than the two- and three-atom transfer in the uranium system. Transfers of five and six fluorine atoms in the uranium system are not observed. These latter observations suggest that there is a kinetic restriction to transferring more than three fluorine atoms in these systems.

The high efficiencies of both SF_6 reactions are in direct contrast with recent results for the reactions of Th^+ and U^+ with CF_4 , where the only product observed at thermal energies is $AnF^+ + CF_3$, with efficiencies near 0.001. These results are obtained even though transferring one to three fluorine atoms from CF_4 to An^+ is strongly exothermic for both Th^+ and U^+ . In those systems, we attributed the inefficient reactivity to a mismatch in the sizes of the atoms compared to CF_4 such that the reaction was proposed to occur by a near-linear $An^+ - F - CF_3$ alignment. A similar comparison for the present systems is shown in Figure 3, where the S-F bond length equals 1.561

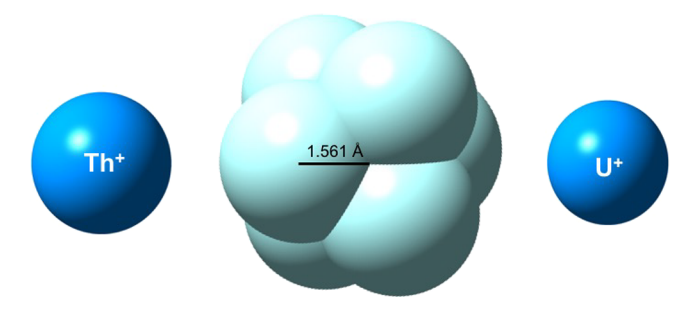


Figure 3. Size comparison of the Th^+ , SF_6 , and U^+ reagents. The S-F bond length is 1.561 Å, and the radii of F, Th^+ , and U^+ are 1.35, 1.59, and 1.38 Å, respectively.

Å⁴³ along with the radii of F, Th⁺, and U⁺ taken as 1.35, 1.59, and 1.38 Å, 12,44 respectively. Presumably, the larger S–F bond length of SF₆ compared with that for C–F in CF₄ (1.315 Å)⁴³ permits the An⁺ to insert into the S–F bond.

At energies above 1 eV, the total cross sections of both SF_6 reaction systems level out, suggesting a conversion to a hard-sphere-like cross section. The hard-sphere cross sections are calculated to be 64 and 58 Ų for Th^+ and U^+ colliding with SF_6 , respectively, using the structural data above. These are shown by the horizontal red line in Figures 1 and 2. In both systems, the observed cross sections are about half of those calculated here, indicating either that the efficiency of bond insertion decreases as the collision energy reaches this hard sphere limit or that the radii of F are overestimated at these higher energies.

 SF_{1-5}^+ **Channels.** As noted above, the exothermic formation of SF_{1-4}^+ is consistent with the reaction enthalpies listed in Table 2. In all cases, the magnitudes of the SF_{6-n}^+ cross sections compared with their AnF_n^+ counterparts are consistent with the relative IEs of the SF_{6-n} and AnF_n products. This comparison is exemplified by the similarity in the UF_4^+ and SF_2^+ cross-section magnitudes, which matches the fact that both UF_4 and SF_2 have identical IEs within experimental uncertainties. Quantitatively, the SF_2^+ cross section is larger than that for UF_4^+ by a factor of ~ 1.5 , which probably means that $\mathsf{IE}(\mathsf{UF}_4)$ is slightly below $\mathsf{IE}(\mathsf{SF}_2) = 10.08 \pm 0.05$ eV, 15,20 toward the lower end of the 10.2 ± 0.3 eV range in the literature.

The SF₅⁺ product is predicted to form endothermically in the reactions $An^+ + SF_6 \rightarrow AnF + SF_5^+$ (An = Th or U). However, the SF₅⁺ product ion cross sections for the reactions of Th+ and U+ with SF₆ display an exothermic behavior and are linearly dependent on the SF₆ pressure. Although there are multiple exothermic secondary processes that may occur between $An^+ + 2SF_6$ reactants (An = Th or U) to form SF₅⁺, likely secondary reactants could be identified by adjusting the observed cross-section behavior for the $E^{-1/2}$ dependence expected for such a secondary reaction. This procedure identified ThF₂⁺ and UF₃⁺ (both abundant primary products) as the most probable candidates involved in the secondary reaction to produce SF₅⁺. For the thorium system, a zeropressure extrapolation of the SF₄⁺ channel reveals that the lowenergy exothermic feature corresponds to a primary reaction, whereas the high-energy endothermic feature is pressuredependent. For the uranium system, the SF₄⁺ channel is pressure-dependent at all energies. The pressure dependence of the SF₄⁺ channels can be explained by secondary reactions between AnF⁺ and SF₆ for the overall reactions An⁺ + $2SF_6 \rightarrow$ $SF_4^+ + AnF_3 + SF_5$, which are exothermic by 418 \pm 27 and 229 ± 26 kJ/mol for Th and U, respectively. The increases observed in the SF₄⁺ channel cross sections parallel the rise with energy in the respective ThF+ and UF+ channels. For the thorium system, it was determined that the rise in the SF₂⁺ cross section at higher energies results from the dissociation of SF₃⁺ to SF₂⁺ + F. Similarly, in the uranium system, there is evidence that SF_3^+ dissociates to SF_2^+ + F at all energies, augmented by secondary collisions.

Prior Ion Trap Results. The GIBMS data at the thermal energy for the reaction of U+ and SF6 are in reasonable agreement with observations previously made for the same reaction studied by Jackson et al. in an ion trap mass spectrometer.²⁵ The earlier ion trap study reported a rate constant of $2.3 \pm 0.7 \times 10^{-10}$ cm³ s⁻¹ and an efficiency of 0.37 ± 0.11 compared to an efficiency near unity measured here. Notably, the ion trap experiments were performed with a He bath gas pressure of 5×10^{-4} Torr, which could potentially remove energy from the initial $U^+(SF_6)$ complex, thereby allowing a more efficient reaction back to reactants. Further, the rate constant measurement reported in the ion trap study was plagued by the presence of residual water, which also reacts efficiently with U+. Therefore, the authors determined the rate constants by comparison with reactions with Ar⁺ as a means of determining the absolute pressure of the SF₆ present. These complications potentially mean that the uncertainty in the absolute rate constant measurement is larger than the stated 30%. As noted above, our total cross-section results were not dependent on the pressure of SF₆, and the observation of a highly efficient reaction for processes that are very strongly

exothermic (Table 2) is certainly reasonable in the absence of a bath gas.

The comparison of the branching ratios among the various products is in much better agreement between the present and previous ion trap studies. Table 3 lists the branching ratios

Table 3. Product Ion Distributions for Reactions of An^+ with SF_6 at 0.03 eV^a

products	Th	U	U (ion trap) ^b
$AnF^+ + SF_5$	0.06 ± 0.01	0.012 ± 0.001	0.05 ± 0.01
$AnF_2^+ + SF_4$	0.37 ± 0.02	0.49 ± 0.02	0.47 ± 0.05
$AnF_3^+ + SF_3$	0.40 ± 0.01	0.38 ± 0.02	0.31 ± 0.03
$AnF_4^+ + SF_2$	N/A	0.015 ± 0.002	< 0.01
$AnF_5^+ + SF$	N/A	N.D.	N.D.
$AnF + SF_5^+$	0.00 ± 0.05^{c}	0.000 ± 0.001^{c}	N.D.
$AnF_2 + SF_4^+$	0.011 ± 0.003	0.000 ± 0.001^{c}	N.D.
$AnF_3 + SF_3^+$	0.11 ± 0.01	0.06 ± 0.02	0.10 ± 0.01
$AnF_4 + SF_2^+$	0.02 ± 0.01	0.031 ± 0.006	0.07 ± 0.01
$AnF_4 + F + SF^+$	0.018 ± 0.006	0.005 ± 0.002	< 0.01

"Average of values taken at low and medium pressure except where noted. N/A, not applicable. N.D., not detected. Branching ratios determined in Ref 25. Extrapolated to zero pressure.

obtained for the observed products after averaging over data sets collected at SF₆ pressures of about 0.05 and 0.1 mTorr. These differ slightly from the results shown in Figures 1 and 2, which show one high-pressure (~0.2 mTorr) data set. Branching ratios from the ion trap data are also listed in Table 3, where it can be seen that both experiments agree that the UF₂⁺ and UF₃⁺ products dominate the product spectrum, with comparable amounts. Likewise, both studies agree that the next two most abundant products are SF₃⁺ and SF₂⁺, with intensity ratios that are similar. We find more UF₄⁺ product than observed in the ion trap study, a result that makes sense given the relative IEs of UF₄ and SF₂, as discussed above. Indeed, the lack of UF₄⁺ in the ion trap study was a subject of considerable discussion. We find less UF+ than the ion trap study, which could be a consequence of the autofragmentation process discussed there (i.e., spontaneous dissociation of highorder UF_n⁺ products); however, it would have been expected that the present experiments, which are performed at very low overall pressures, might be subject to more of this process than the ion trap experiments where a bath of He is also present. Instead, we speculate either that UF+ reacted with the background H₂O in the ion trap experiment or that collisional cooling in the ion trap slowed the kinetics of fluorine atom transfer, thereby enhancing the formation of the UF+ + SF5 product channel.

CONCLUSIONS

Reactions of thorium and uranium cations with SF_6 were observed to form ThF_{1-3}^+ , UF_{1-4}^+ , and SF_{1-4}^+ species in exothermic, barrierless processes, in agreement with the literature thermochemistry. Reactions of both Th^+ and U^+ with SF_6 proceed very efficiently at all energies. Notably, even though exothermic (Table 2), the transfer of five and six fluorine atoms from sulfur to uranium was not observed, and there is evidence for a relatively inefficient transfer of four fluorine atoms in both systems. These observations are consistent with a kinetic limitation in the transfer of this many ligands during the lifetime of the collision complex. Overall, results for the reaction of U^+ with SF_6 are similar to

those obtained in an earlier ion trap study;²⁵ however, the efficiency determined here is higher (98%) than that obtained in the ion trap study (37%), presumably a result of the very different conditions used. Additional processes that occur at higher energies were identified here and include the decomposition of AnF₃⁺ to AnF⁺ + F₂, fragmentation of SF₃⁺ to SF_2^+ + F for the thorium and uranium systems, and reaction of AnF⁺ with SF₆ to yield SF₄⁺ + AnF₃. Although the formation of SF_5^+ by the reaction $An^+ + SF_6 \rightarrow SF_5^+ + AnF$ is endothermic for both An = Th and U, the SF₅⁺ product was observed for both systems at the lowest energies. Analysis of the pressure dependences of these product channels revealed that SF_5^+ forms exothermically through secondary reactions. ThF₂⁺ and UF₃⁺ were identified as the probable species that go on to react with SF_6 to form SF_5^+ by adjusting for the additional $E^{-1/2}$ dependence of the SF_5^+ cross section and matching the shape of the cross section to that of the appropriate ionic precursor.

ASSOCIATED CONTENT

Supporting Information

The Supporting Information is available free of charge at https://pubs.acs.org/doi/10.1021/acs.jpca.2c02090.

Figures showing the pressure dependence of the SF_4^+ and SF_5^+ product ions from reactions with $Th^+ + SF_6$ and of the SF_2^+ , SF_3^+ , SF_4^+ , and SF_5^+ product ions from reactions with $U^+ + SF_6$ (PDF)

AUTHOR INFORMATION

Corresponding Author

P.B. Armentrout — Department of Chemistry, University of Utah, Salt Lake City, Utah 84112-0850, United States; orcid.org/0000-0003-2953-6039; Email: armentrout@chem.utah.edu

Authors

Amanda R. Bubas — Department of Chemistry, University of Utah, Salt Lake City, Utah 84112-0850, United States

Anna C. Iacovino — Department of Chemistry, University of Utah, Salt Lake City, Utah 84112-0850, United States;

Present Address: PPG Coatings Innovation Center, 4325

Rosanna Drive, Allison Park, Pennsylvania 15101, USA

Complete contact information is available at: https://pubs.acs.org/10.1021/acs.jpca.2c02090

Notes

The authors declare no competing financial interest.

ACKNOWLEDGMENTS

This work is supported by the Heavy Element Chemistry Program, Office of Basic Energy Sciences, U.S. Department of Energy, through Grant DE-SC0012249. This work was also supported by the University of Utah NSF REU program awarded to A.C.I. (Grant CHE-1659579).

REFERENCES

- (1) Bahri, C. N. A. C. Z.; Majid, A. A.; Al-Areqi, W. M. In Advantages of Liquid Fluoride Thorium Reactor in Comparison with Light Water Reactor; AIP Conf. Proc., AIP Publishing LLC: 2015; p 040001.
- (2) Heriot, I. Uranium Enrichment by Centrifuge; Report EUR 11486; Commission of the European Communities: Brussels 1988.
- (3) Edelstein, N. M.; Fuger, J.; Katz, J. J.; Morss, L. R., Summary and Comparison of Properties of the Actinide and Transactinide

- Elements. In *The Chemistry of the Actinide and Transactinide Elements*; Springer: 2010; pp. 1753–1835.
- (4) Fuger, J.; Parker, V.; Hubbard, W.; Oetting, F. Chemical Thermodynamics of Actinide Elements and Compounds. Part 8. The Actinide Halides; Int. Atomic Energy Agency: Vienna, Austria, 1983.
- (5) Lau, K. H.; Hildenbrand, D. L. Thermochemical Properties of the Gaseous Lower Valent Fluorides of Uranium. *J. Chem. Phys.* **1982**, 76, 2646–2652.
- (6) Lau, K. H.; Brittain, R. D.; Hildenbrand, D. L. High Temperature Thermodynamic Studies of Some Gaseous Thorium Fluorides. *J. Chem. Phys.* **1989**, *90*, 1158–1164.
- (7) Hildenbrand, D. L.; Lau, K. H. Redetermination of the Thermochemistry of Gaseous UF₅, UF₂, and UF. *J. Chem. Phys.* **1991**, *94*, 1420–1425.
- (8) Antonov, I. O.; Heaven, M. C. Spectroscopic and Theoretical Investigations of UF and UF⁺. *J. Phys. Chem. A* **2013**, *117*, 9684–9694
- (9) Barker, B. J.; Antonov, I. O.; Heaven, M. C.; Peterson, K. A. Spectroscopic Investigations of ThF and ThF⁺. *J. Chem. Phys.* **2012**, *136*, 104305.
- (10) Dyke, J. M.; Fayad, N. K.; Morris, A.; Trickle, I. R.; Allen, G. C. A Study of the Electronic Structure of the Actinide Tetrahalides UF₄, ThF₄, UCl₄ and ThCl₄ Using Vacuum Ultraviolet Photoelectron Spectroscopy and SCF-X α Scattered Wave Calculations. *J. Chem. Phys.* **1980**, 72, 3822–3827.
- (11) Irikura, K. K. Gas-Phase Energetics of Thorium Fluorides and Their Ions. J. Phys. Chem. A 2013, 117, 1276–1282.
- (12) Bubas, A. R.; Owen, C. J.; Armentrout, P. B. Reactions of Atomic Thorium and Uranium Cations with CF₄ Studied by Guided Ion Beam Tandem Mass Spectrometry. *Int. J. Mass Spectrom.* **2022**, 472, 116778.
- (13) Bartmess, J. E. Thermodynamics of the Electron and the Proton. J. Phys. Chem. 1994, 98, 6420-6424.
- (14) Hildenbrand, D. Thermochemistry of Gaseous UF₅ and UF₄. *J. Chem. Phys.* **1977**, *66*, 4788–4794.
- (15) Lias, S. G. *Ionization Energy Evaluation*; National Institute of Standards and Technology: Gaithersburg MD, 2001; Vol. NIST Standard Reference Database Number 69, p (http://webbook.nist.gov).
- (16) Chase, M. W. NIST-JANAF Thermochemical Tables. *Journal of Physical and Chemical Reference Data*; American Institute of Physics, *Monograph No.* 9 1998, 4th Edition, 1–1963.
- (17) Fisher, E. R.; Kickel, B. L.; Armentrout, P. B. Collision-Induced Dissociation and Charge Transfer Reactions of SF_x^+ (x = 1-5): Thermochemistry of Sulfur Fluoride Ions and Neutrals. *J. Chem. Phys.* **1992**, *97*, 4859–4870.
- (18) Rodgers, M. T.; Ervin, K. M.; Armentrout, P. B. Statistical Modeling of Collision-Induced Dissociation Thresholds. *J. Chem. Phys.* **1997**, *106*, 4499–4508.
- (19) Armentrout, P. B.; Ervin, K. M.; Rodgers, M. T. Statistical Rate Theory and Kinetic Energy-Resolved Ion Chemistry Theory and Applications. *J. Phys. Chem. A* **2008**, *112*, 10071–10085.
- (20) Cheung, Y.-S.; Chen, Y.-J.; Ng, C. Y.; Chiu, S.-W.; Li, W.-K. Combining Theory with Experiment: Assessment of the Thermochemistry of SF_n , SF_n^+ , and SF_n^- , n=1-6. J. Am. Chem. Soc. **1995**, 117, 9725–9733.
- (21) Evans, M.; Ng, C. Y.; Hsu, C.-W.; Heimann, P. A High Resolution Energy-selected Kinetic Energy Release Study of the Process $SF_6 + h\nu \rightarrow SF_5^+ + F + e^-$: Heat of Formation of SF_5^+ . *J. Chem. Phys.* **1997**, *106*, 978–981.
- (22) Sieck, L. W.; Ausloos, P. J. The Ionization Energy of SF_5 and the SF_5 –F Bond Dissociation Energy. *J. Chem. Phys.* **1990**, 93, 8374–8378.
- (23) Irikura, K. K. Structure and thermochemistry of sulfur fluorides SF_n (n = 1-5) and their ions SF_n^+ (n = 1-5). *J. Chem. Phys.* **1995**, 102, 5357–5367.
- (24) Bauschlicher, C. W.; Ricca, A. Accurate Heats of Formation for SF_n , SF_n^+ , and SF_n^- for n=1-6. J. Phys. Chem. A **1998**, 102, 4722–4727.

- (25) Jackson, G. P.; Gibson, J. K.; Duckworth, D. C. Gas-Phase Reactions of Bare and Ligated Uranium Ions with Sulfur Hexafluoride. *J. Phys. Chem. A* **2004**, *108*, 1042–1051.
- (26) Loh, S. K.; Hales, D. A.; Lian, L.; Armentrout, P. B. Collision-Induced Dissociation of Fe_n^+ (n=2-10) with Xe: Ionic and Neutral Iron Cluster Binding Energies. *J. Chem. Phys.* **1989**, *90*, 5466–5485.
- (27) Schultz, R. H.; Armentrout, P. B. Reactions of N_4^+ with Rare Gases from Thermal to 10eV center-of-mass energy: Collision-Induced Dissociation, Charge Transfer, and Ligand Exchange. *Int. J. Mass Spectrom. Ion Processes* **1991**, 107, 29–48.
- (28) Kickel, B. L.; Armentrout, P. B. Reactions of Fe⁺, Co⁺ and Ni⁺ with Silane. Electronic State Effects, Comparison to Reactions with Methane, and M⁺-SiH_x (x = 0-3) Bond Energies. *J. Am. Chem. Soc.* **1995**, *117*, 764–773.
- (29) Kickel, B. L.; Armentrout, P. B. Guided Ion Beam Studies of the Reactions of Ti⁺, V⁺, and Cr⁺ with Silane. Electronic State Effects, Comparison to Reactions with Methane, and M⁺-SiH_x (x = 0-3) Bond Energies. *J. Am. Chem. Soc.* **1994**, *116*, 10742–10750.
- (30) Kickel, B. L.; Armentrout, P. B. Guided Ion Beam Studies of the Reactions of Mn^+ , Cu^+ , and Zn^+ with Silane. M^+ -SiH_x (x = 0-3) Bond Energies. *J. Phys. Chem.* **1995**, *99*, 2024–2032.
- (31) Kickel, B. L.; Armentrout, P. B. Guided Ion Beam Studies of the Reactions of Group 3 Metal Ions (Sc^+ , Y^+ , La^+ , and Lu^+) with Silane. Electronic State Effects, Comparison to Reactions with Methane, and M^+ -SiH $_x$ (x=0-3) Bond Energies. *J. Am. Chem. Soc.* **1995**, *117*, 4057–4070.
- (32) Sievers, M. R.; Chen, Y.-M.; Elkind, J. L.; Armentrout, P. B. Reactions of Y⁺, Zr⁺, Nb⁺, and Mo⁺ with H₂, HD, and D₂. *J. Phys. Chem.* **1996**, *100*, 54–62.
- (33) Clemmer, D. E.; Chen, Y.-M.; Khan, F. A.; Armentrout, P. B. State-Specific Reactions of Fe $^+$ (a 6 D, a 4 F) with D $_2$ O and Reactions of FeO $^+$ with D $_2$. *J. Phys. Chem.* **1994**, *98*, 6522–6529.
- (34) Cox, R. M.; Armentrout, P. B.; de Jong, W. A. Reactions of Th⁺ + H₂, D₂, and HD Studied by Guided Ion Beam Tandem Mass Spectrometry and Quantum Chemical Calculations. *J. Phys. Chem. B* **2016**, 120, 1601–1614.
- (35) Zhang, W.-J.; Demireva, M.; Kim, J.; de Jong, W. A.; Armentrout, P. B. Reactions of U⁺ with H₂, D₂, and HD Studied by Guided Ion Beam Tandem Mass Spectrometry and Theory. *J. Phys. Chem. A* **2021**, *125*, 7825–7839.
- (36) Gerlich, D. Inhomogeneous rf Fields: A Versatile Tool for the Study of Processes with Slow Ions. In *Advances in Chemical Physics*; Ng, C.-Y.; Baer, M., Eds.; Wiley, 1992; Vol. 82, pp. 1–176, DOI: 10.1002/9780470141397.ch1.
- (37) Ervin, K. M.; Armentrout, P. B. Translational Energy Dependence of $Ar^+ + XY \rightarrow ArX^+ + Y$ ($XY = H_2, D_2, HD$) from Thermal to 30 eV c.m. *J. Chem. Phys.* **1985**, *83*, 166–189.
- (38) Hales, D. A.; Lian, L.; Armentrout, P. B. Collision-Induced Dissociation of Nb_n^+ (n = 2 11): Bond Energies and Dissociation Pathways. *Int. J. Mass Spectrom. Ion Processes* **1990**, *102*, 269–301.
- (39) Daly, N. R. Scintillation Type Mass Spectrometer Ion Detector. Rev. Sci. Instrum. 1960, 31, 264–267.
- (40) Langevin, M. P. Une Formule Fondamentale de Theorie Cinetique. *Ann. Chim. Phys. Ser.* **1905**, *8*, 245–288.
- (41) Gioumousis, G.; Stevenson, D. P. Reactions of Gaseous Molecule Ions with Gaseous Molecules. V. Theory. *J. Chem. Phys.* **1958**, *29*, 294–299.
- (42) Gussoni, M.; Rui, M.; Zerbi, G. Electronic and Relaxation Contribution to Linear Molecular Polarizability. An Analysis of the Experimental Values. *J. Mol. Struct.* **1998**, 447, 163–215.
- (43) Johnson, R. D., III NIST Computational Chemistry Comparison and Benchmark Database; http://cccbdb.nist.gov/ (accessed April 12, 2018).
- (44) Wilson, R. G.; Brewer, G. R. Ion Beams with Applications to Ion Implantation; Wiley: New York, 1973.